



An Evaluation of Cots-Based Radar for Very Small Drone Sense and Avoid Application

Khairul Khaizi Mohd Shariff^{1*}, Suraya Zainuddin², Nur Emileen Abd Rashid¹, Rizal Effendy Mohd Nasir³, Wirachman Wisnoe³, Saiful Aman Sulaiman⁴

¹Microwave Research Institute,
Universiti Teknologi MARA, Shah Alam, Selangor, 40450, MALAYSIA

²Faculty of Electrical and Electronic Engineering Technology,
Universiti Teknikal Malaysia Melaka, Hang Tuah Jaya, Melaka 76100, MALAYSIA

³School of Electrical Engineering, College of Engineering,
Universiti Teknologi MARA, 40450 Shah Alam, Selangor, MALAYSIA

³School of Electrical Engineering, College of Engineering,
Universiti Teknologi MARA, 40450 Shah Alam, Selangor, MALAYSIA

⁴Malaysia Institute of Transport (MITRANS)
Universiti Teknologi MARA, 40450 Shah Alam, Selangor, MALAYSIA

*Corresponding Author

DOI: <https://doi.org/10.30880/ijie.2022.14.01.035>

Received 21 July 2021; Accepted 08 November 2021; Available online 07 March 2022

Abstract: The use of very small unmanned aerial vehicles (UAVs) are increasingly common these days but its applications are limited to the pilot line-of-sight view. To extend its use beyond the pilot view, UAVs need to be equipped sense and avoid (SAA) system to avoid potential collisions. However, the development of SAA for very small drones is still in the infancy stage mainly due to the high cost of design and development for reliable range sensors. Recent developments of very small size and lightweight commercial off-the-shelf (COTS)-based radar systems may become a crucial element in very small drone applications. These types of radars are primarily developed for industrial sensing but can be adapted for applications such SAA. Thus, this paper contributes to the survey of a miniature and lightweight radar sensor to assist the SAA development. The focus of this paper is to analyse the eligibility of a COTS-based radar in detecting very small drones. For this purpose, we used a frequency-modulated continuous radar (FMCW) developed by Infineon Technologies. Field test results show the real-time capability of the radar sensor to detect the very small drones within ± 0.5 meters in static and dynamic conditions.

Keywords: COTS radar, radar detection, sense and avoid, UAV, transportation, high frequency

1. Introduction

Very small UAV or ordinarily called drones are typically less than 2 kilograms, and costing about a few hundreds of dollars [1]. Drones are prevalent, they are useful in many applications ranging from recreational and commercial purposes including photography, surveillance, and delivery of light packages. For these reasons, consumer drones are gaining

popularity. it is expected the use of drones will continue to grow rapidly in the coming years with values expected to more than USD 10 billion in years 2035 [2].

In most cases, drones are control by the pilot which maintains the flight within the visual line-of-sight (VLOS) and therefore ensures the safety of the drones including avoiding potential collision with other drones. Nonetheless, some applications such as package delivery may require operating beyond visual line-of-sight (BVLOS) [3]. In this case, the drones themselves need some autonomy to ensure their flight safety.

Sense and Avoid (SAA) is an autonomous technology that allows drones to sense the surrounding environment for obstacles such as flying objects and executing necessary alterations in their trajectory to avoid a potential collision. A typical SAA system consists of two main components that are 1) self-separation component that sense assures a safe separation from a potential hit and 2) collision avoidance component that operates when the safe separation is lost. Undeniably, the SAA system is a key which will unlock many BVLOS applications.

A reliable range sensor is vital for SAA system. For this reason, several on-board sensors have been investigated. Some typical sensors are radar [4]–[6], optical [7]–[9], acoustic [10]–[12] and lidar sensor [13]. Though, radar sensor has several important advantages over other types of sensors for SAA system. Its main advantage is the ability to perform target distance measurements under rain, dust, and fog conditions. Another advantage is that the target range and size measurement tend to be less computationally intensive than the optical and acoustic systems which often use complex machine learning processing.

While radar sensor has been explored for SAA system, they are overwhelmingly dedicated for to medium and large-sized drones [14]–[16]. To date, research efforts in radar-based SAA system to detect very small drones (weight < 2 kilograms) is still few. The few problems that are holding back the development progress are physical issues such as weight, size, power consumption, and cost of development.

For all of the above problems, COTS-based radars can offer attractive design solutions for developing the SAA system. They offer affordable and timely provision compared to the traditional development activities such as developing application-specific integrated circuits (ASICs). COTS-based radar features basic radar elements; radiofrequency (RF) front-end and signal processing system to detect targets. Moreover, this technology can be purchase “off-the-shelf” and provided by many vendors. Some examples of COTS-based radars include distance2go [17], uRAD [18] and IMST [19]. They are frequency-modulated continuous-wave radar (FMCW) that can estimate targets range and velocity in the observation volume. Currently, almost all COTS-based radar operates in the in the industrial, scientific, and medical (ISM) band mainly at two frequency bands of 24 GHz and 77 – 81 GHz [20]. Depending on the manufacturer and targeted applications, these radar differs in the level of functional modifiability, packaging (dimension and weight) and operating frequency.

In this paper, we evaluate the eligibility of a COTS-based radar for SAA application. The scope of this paper is to analyse the capability of a COTS-based radar to detect very small drones in static and dynamic flying conditions. This paper is organised as follows: Section II introduces the COTS radar and radar measurement, Section III deals with the field test and illustrate the main results and findings. Finally, Section IV concludes the work in this paper.

2. Distance2go Radar

2.1 Technical Description

We use a COTS radar named distance2go developed by Infineon Technologies. This radar is lightweight and miniature, it weighs 25.1 grams and has a width and length of 36 mm and 45 mm, and operates at frequency of 24 GHz. The radar is powered using a 5 V DC supply. The radar system consists of four main parts: 1) The radio frequency (RF), 2) Frequency control and Phase lock loop (PLL), 3) the analogue amplifier, and 4) the digital unit. Further details on each of the radar parts can be found in [21]. Fig. 1 shows the top and bottom of the radar module. It consists of a mainboard which contains the radar system and a debugger board which function to program the radar microcontroller.

The radar also equipped with three software tools: 1) flashing tool, 2) visualization tool and 3) firmware development tool. The flashing tools function to load firmware to the radar using a standard computer. The visualization tool provides real-time visual visualization of target data and also as an interface for customising radar parameters, including transmit frequency, power, receiving gain, and FMCW frame and chirp settings. Finally, the firmware development tools enable user to develop or alter the radar firmware.

Retrieving target detection data is performed by connected the radar to a computer through a USB connector. Data can be collected either in raw information capture by the radar, time-domain formatted data (*.tdd), frequency domain formatted data (*.tdd), or target data in which target detection is processed by the tool itself (Infineon format: *.trg).



Fig. 1 - Distance2go radar

2.2 FMCW Radar Target Range Estimation

Fig. 2 below illustrate the operating principle of FMCW radar. The waveform consists of up-chirp repeated every cycle. The period of one chirp, bandwidth, and carrier frequency are denoted by BW , t_p and f_0 respectively. This sawtooth waveform can provide the ability to detect the target range from the propagation delay within a single frequency ramp. The range of a target can be calculated by

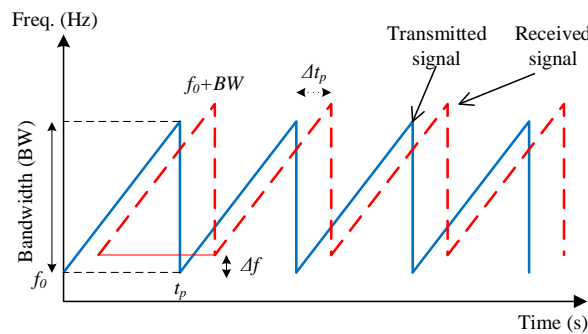


Fig. 2 - The operating principle of FMCW radar

$$R = \frac{ct_p}{2B} \Delta f \tag{1}$$

where Δf is the difference between transmit and received frequency or simply called the beat frequency, t_p is the sweep time, B is the bandwidth, and c is the speed of light. Equation 1 shows that with larger frequency bandwidth, the radar provides finer range resolution. The range resolution is given by

$$\Delta r = \frac{c}{2B} \tag{2}$$

The beat frequency of the radar echo can be estimated by generating frequency domain samples using FFT. The error threshold for the range estimation is defined at 1 m based on the maximum error equation as follows.

$$\Delta R = \frac{ct_p f_s}{2BN_s} \tag{3}$$

In which, f_s is the sampling frequency, and N_s is the number of samples.

3. Methodology

The initial plan was to assemble the Distance2go radar on a drone that can fly the radar. Nonetheless, we decided not to mount the radar on a drone in the actual experiment. This decision was taken to ensure that the complex drone motions, i.e., vibration, are not accounted for in the evaluation process. Instead, we mounted the radar on a fixed pole.

A measurement campaign was carried out to evaluate the capability of the distance2go radar in detecting very small drones. Fig. 3 shows the actual experimental setup. The radar was mounted at the height of $h_r = 2.5$ m from the ground. Two sets of measurements were performed by illuminating the drones in still and moving conditions. For still condition, the drone is hovering at a fixed height of $h_d = 2.5$ m. Conversely, for moving mode, the radar was made flying at low speed (< 10 km/h) and crossing the radar illumination space as indicated with a yellow dashed line in Fig 3. The initial

distance, d_0 of the drone before crossing the baseline is $d_0 = 5$ m. In order to guarantee a straight flight of the drone, the drone straight flight mode was used.

In both flying conditions (static and moving), the radar time-domain in-phase (I) and quadrature (Q) signal (Infineon format: *.tdd), the frequency-domain (Infineon format: *.fdd) and the target file (Infineon format: *.trg), are recorded in the computer through the USB. Consequently, offline processing was performed on the captured file for further analyses.

The parameters of the radar were set via the graphical user interface (GUI) supplied by Infineon. It is worth mentioning that the stated theoretical range detection for a target with radar cross-section (RCS) of 1 m^2 is 15 meters. For very small drone detection, the expected RCS would be less than 1, so the detection range will be less than the specified maximum detection range. Within this decision, we set the radar parameters to the following values:

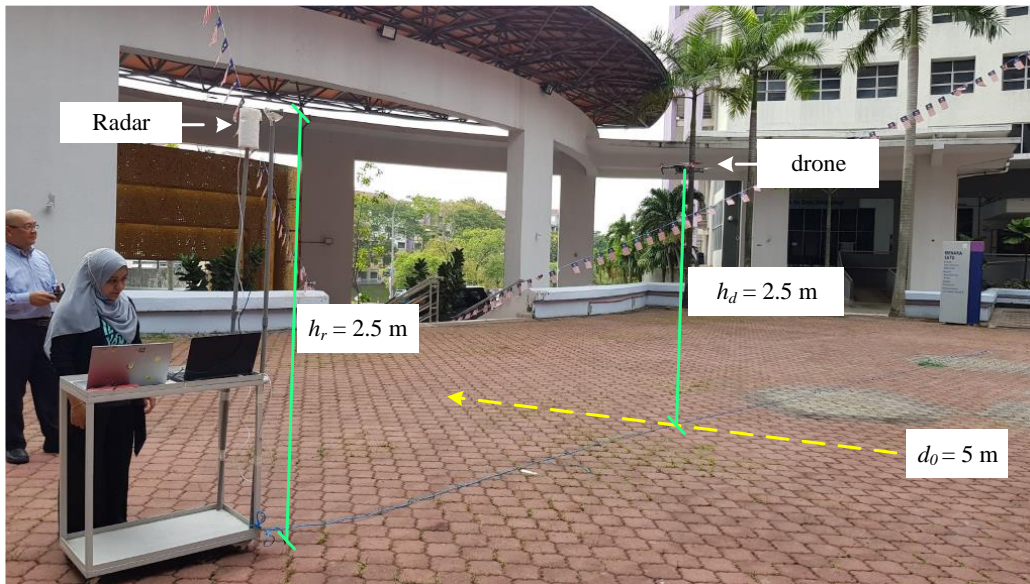


Fig. 3 - Experimental setup and test site

Table 1 - Radar parameters in the evaluation

Parameter	Description
Frequency Modulation	Linear up-chirp (sawtooth)
Ramp duration	1.5 milliseconds
No of sample	256
Ramp bandwidth	BW1: 150 MHz (f_c : 20.035 GHz) BW2: 200 MHz (f_c : 20.025 GHz)
IF gain	34 dB
Sampling frequency	170667 Hz (no. of samples \times 1000 \times 1000/1 chirp time)

The module operated at a low gain mode of a total IF gain = 34 dB with a 3-dB frequency response between 14 kHz and 120 kHz, sufficient for short-range target detection less than 15 m. Therefore, utilising 150 MHz bandwidth (BW1) and 200 MHz bandwidth (BW2), the achieved range resolution is 1 m and 0.75 m, respectively.

Two radar targets of very small drones were used in this experiment. Table 2 describes the drones utilised in this exercise.

Table 2 - Radar parameters in the evaluation

Drone type	Description
Drone A	 <p>DJI Mavic Pro – 734-gram mass, 354 mm diagonal length (excluding propeller), Dimensions, unfolded: 322×242×84 mm (L×W×H)</p>
Drone B	 <p>DJI Mavic Mini – 249-gram mass, 213 mm diagonal length (excluding propeller), Unfolded 159×202×55 mm (L×W×H)</p>

4. Experimental Results and Discussions

4.1 Time Domain Analysis

Firstly, an analysis was carried out over the beat signal in a time-domain utilizing the Infineon *.tdd file. Fig. 4 depicts the example of beat signal in time domain taken for Drone A and Drone B at 3 m target’s range.

No significant change was observed on the beat signal in detecting two different sizes of drones (Drone A and Drone B). However, there is a difference in signal amplitude observed between BW1 and BW2. BW1 with a carrier frequency of 20.035 GHz produced a lower beat signal amplitude than BW2 with a slightly lower operating frequency. The scenario can be explained by a higher path loss that attenuates the transmitting signal energy when a higher operating frequency is applied [22].

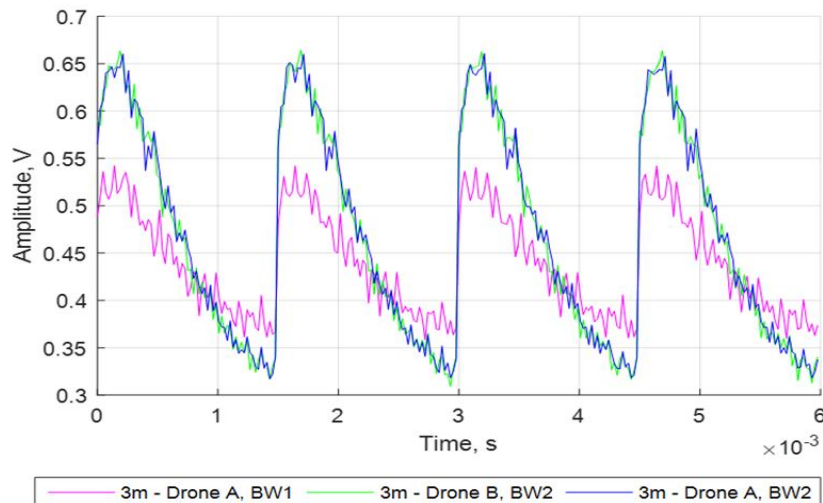


Fig. 4 - Example of beat signal in time domain taken for Drone A and Drone B at 3 m target’s range

4.2 Frequency Spectrum Analysis

Next, a further assessment was executed over the beat signal FFT spectrum utilizing Infineon *.fdd file. Analysis in the frequency domain provided more apparent peaks due to a beat signal is obtained through a frequency change between the received signal and reference signal.

Fig. 5 illustrates the local maxima peak of beat frequencies within the highlighted region. The highlighted region is the frequency of interest during target measurement, between 1777 Hz (equal to 2 m) and 8889 Hz (equal to 10 m). Data was taken over measurement using 200 MHz ramp bandwidth.

The frequency of interest range is defined between 2 m to 10 m to accommodate the target range of 3 m, 6 m, and 9 m, together with the allowable error threshold. Details of the threshold selection will be explained in the next section. Each marker presents the beat frequency for the estimated range at each measured distance. The difference between the actual and estimated range is tabulated in Table 3. Fig. 5 and Table 3 show consistent readings between data 1 and data 2 for each target range measurement.

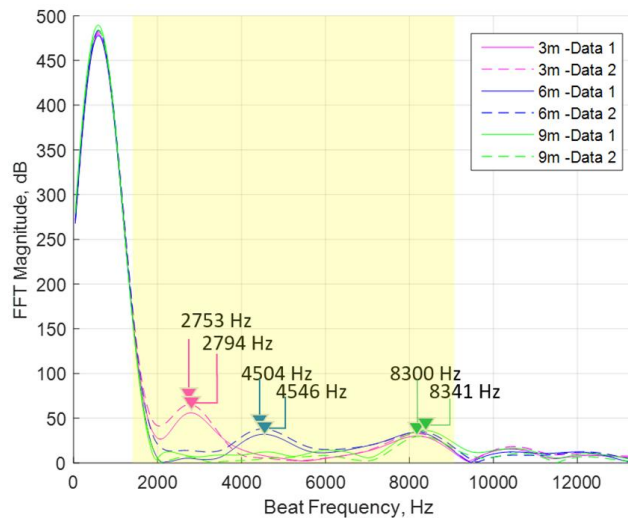


Fig. 5 - Example of FFT spectrum for target = Drone A

Table 3 - Comparison of detected target and actual target

Actual Target Range (m)	Data	Beat Frequency (Hz)	Estimate Target Range (m)	Difference (%)	Difference (%)
3	1	2794	3.144	0.144	4.8%
	2	275	3.097	0.097	3.23%
6	1	4546	5.114	0.86	14.8%
	2	4504	5.067	0.067	1.34%
9	1	8341	9.384	0.384	4.27%
	2	8300	9.338	0.338	3.76%

4.3 Range Estimation Analysis on Different Target Motion

Drone A estimated range was observed for 50 iterations at 3m, 6m, and 9m over a static and moving motion. Fifty iterations were chosen to fit the number of data captured during the target was moving through the flight path.

Measurements were taken at 3 m, 6 m, and 9 m. The selection of target range was to allow the maximum error threshold based on Equation (3). From this equation, the maximum range error is 1 m for a 150 MHz bandwidth and 0.75 m for a 200 MHz bandwidth. Thus, a 1 m threshold was chosen for the campaign’s evaluation and the threshold is not overlapping between all three ranges measured. Table 4 presents the range threshold for each measured range.

Table 4 - Range threshold for measured target distance

Actual Target Range (m)	Range Error Threshold ($\pm 1m$)	
	Min. Range (m)	Max. Range (m)
3	2	4
6	5	7
9	8	10

During the analysis, the undetected target was defined as 0 m. Figure 6 represents the estimated range for Drone A at 3 m, 6 m, and 9 m for a static target (a) and a moving target (b), where it displays more consistency in range estimation for a static target than a moving target. It is observed through the dispersion of estimated range data for each target distance. Besides, the target is undetected more frequently during moving motion compared to static, through data presented by the 'zero' range. It was due to the doppler existence by a moving target which produces a frequency shifting of a received signal. In addition, a target RCS also relies on the target speed and provides a change in RCS value during the movement from the observing radar perspective. In addition, the further a target from the radar, the further dispersion resulted from the actual target baseline.

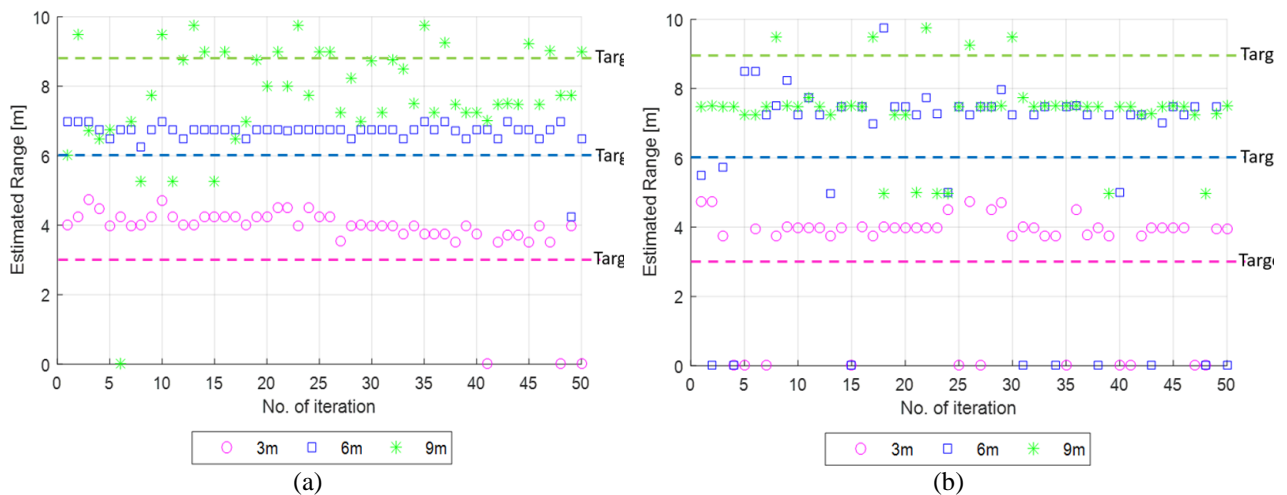


Fig. 6 - Estimated range for Drone A (iteration = 50) (a) static and (b) moving, at various target range.

4.4 Range Estimation Analysis using Different Frequency Sweep Range

Next, an analysis was performed to observe the effect of utilising different frequency sweep range or different bandwidth size. For this campaign, 150 MHz (BW1) and 200 MHz (BW2) were applied.

Fig. 7 illustrates dispersion of estimated range with Drone A at 3 m (a), 6 m (b), and 9 m (c). The highlighted area is the range threshold with ± 1 m error.

At 3 m target's distance, a static target detection resulting in 82% of distribution within the allowable threshold and 76% for a moving target for both bandwidth setups as Table 5. A moving target from utilising both setups producing frequent readings of the undetectable target presented by zero readings.

At 6 m target's distance, a static target with BW1 and BW2 implementation display a concentrated disperse within the range threshold at 82% and 80%, respectively. Meanwhile, a moving target displays a consistent reading, but most are out of the threshold, which is more than 50% spreading is out of the region.

Finally, a similar distribution was observed at the 9 m target's distance with a static target, resulting in a higher distribution within the allowable region than a moving target. The graph also presents that data spread further from the baseline compared to the 6 m target's reading. Target motion increases the difficulty of target detection as it affects the target's RCS [23].

Overall, BW2 produces a better reading for moving and static targets attributable to the better signal energy received due to its slightly lower transmitting frequency. Besides, a nearer target to the radar resulting in a better range estimation as the reflected signal energy received is higher compared to further distance resulted from the path loss.

Table 5 - Distribution of range estimation for setup utilising various bandwidth in estimating moving and static targets

Target distance (m)	Scenario	No. of range estimation		
		Within threshold	Out of threshold	Percentage estimation within threshold
3	BW1, moving	38	12	76%
	BW1, static	41	9	82%
	BW2, moving	38	12	76%
	BW2, static	41	9	82%
6	BW1, moving	7	43	14%
	BW1, static	41	9	82%
	BW2, moving	11	39	22%
	BW2, static	40	10	80%
9	BW1, moving	5	45	10%
	BW1, static	17	33	34%
	BW2, moving	7	43	14%
	BW2, static	30	20	60%

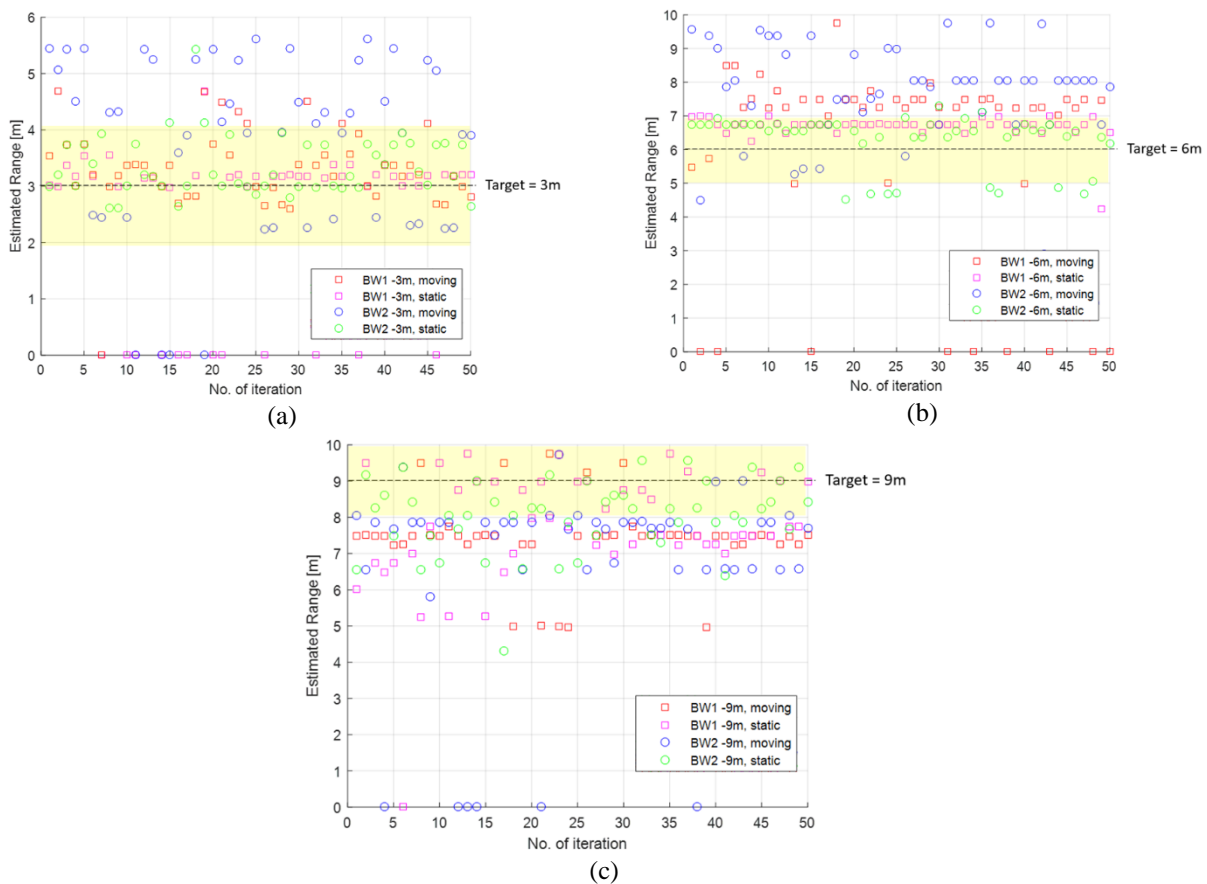


Fig. 7 - Estimated range for Drone A (iteration = 50) (a) static and (b) moving, at various target range.

4.5 Range Estimation Analysis on Different Target Size

Finally, an experiment was conducted over a small size target (Drone B). During the exercise, it was noticed that Drone B was visible at 3 m and was undetected for 6 m and 9 m due to its small size.

Figure 8 depicts the distribution of range estimated for two types of drones. With a larger size, Drone A produced a more consistent reading in both conditions, static and moving motion.

Table 6 tabulated the distribution of range estimation for moving and static targets with various target’s sizes. In a static target scenario, Drone A produces 82%, and Drone B produces 76%, for estimation within the threshold. Meanwhile, the bigger drone resulted in 76% data in the allowable range, and the smaller drone is only at 38%. A target’s

size is one of the parameters impacting the radar cross-section (RCS). The smaller target size produces a smaller RCS, which caused the target of interest to be hard to be detected.

Drone B produces data that disperse far from the baseline in the moving target scenario, and most of the data was out of the threshold region, as Figure 8 (b). It is aware due to RCS dependency on a target’s size and a target’s motion. By having a smaller moving target, the difficulty of target estimation increase.

Table 6 - Distribution of range estimation for moving and static targets with various size

Target distance (m)	Scenario	No. of range estimation		
		Within threshold	Out of threshold	Percentage estimation within threshold
3	Drone A, static	41	9	82%
	Drone B, static	38	12	76%
	Drone A, moving	38	12	76%
	Drone B, moving	19	31	38%

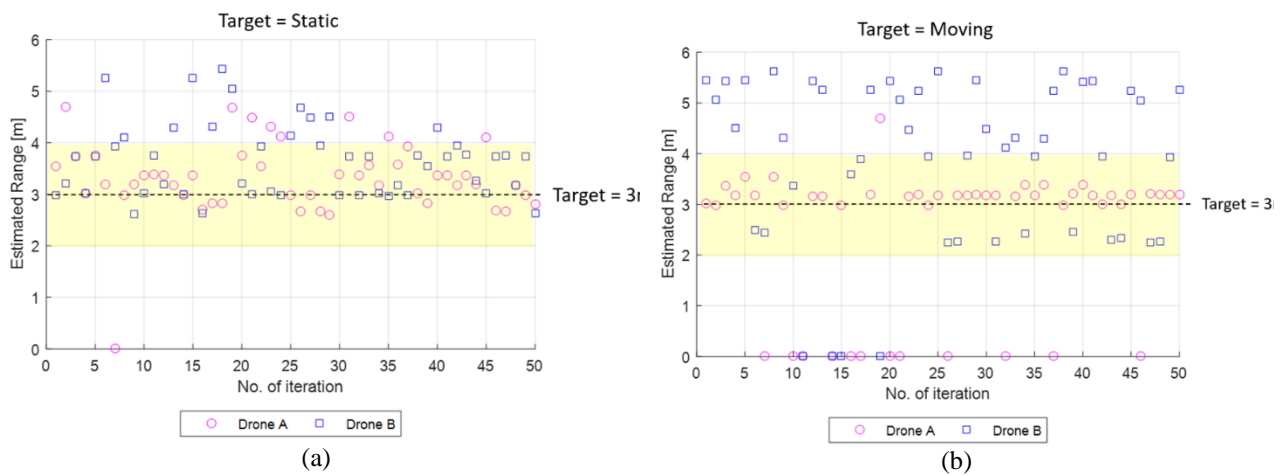


Fig. 8 - Estimated range for Drone A and Drone B (iteration = 50) (a) static and (b) moving, at target range = 3 m

5. Conclusion

The ability of a miniature COTS radar to detect a very small UAV target has been demonstrated in this paper. A popular COTS FMCW radar: distance2go radar by Infineon Technologies were evaluated through series of field experiments. Results present that the Distance2go radar was able to detect small UAV in static and dynamic conditions with 0.5-meter accuracy. Besides, it was observed that the received signal magnitude dropped with distance, which caused the range estimation accuracy to degrade. Targets moving motion and small size also caused the performance to deteriorate as both parameters were impacting the target RCS. Overall, this paper shows that the COTS-based development was an economical choice compared to traditional development, which is a specific context for SAA. However, the proposed solution comes with a trade-off between cost and accuracy.

Acknowledgement

This research is fully supported by MITRANS grant, 600-RMC/MITRANS_IRES 5/3(002/2020). The authors would like to thank Research Management Institute (RMI) and Universiti Teknologi MARA for all the supports.

References

[1] A. la Cour-Harbo, ‘Mass threshold for “harmless” drones’, *Int. J. Micro Air Veh.*, vol. 9, no. 2, pp. 77–92, Jun. 2017, doi: 10.1177/1756829317691991.
 [2] ‘SESAR Joint Undertaking : “European Drones Outlook StudyUnlocking the value for Europe’, Publications Office of the EU, Nov. 2016.

- [3] L. Davies, R. C. Bolam, Y. Vagapov, and A. Anuchin, 'Review of Unmanned Aircraft System Technologies to Enable Beyond Visual Line of Sight (BVLOS) Operations', in *2018 X International Conference on Electrical Power Drive Systems (ICEPDS)*, Oct. 2018, pp. 1–6. doi: 10.1109/ICEPDS.2018.8571665.
- [4] C. Schüpbach, C. Patry, F. Maasdorp, U. Böniger, and P. Wellig, 'Micro-UAV detection using DAB-based passive radar', in *2017 IEEE Radar Conference (RadarConf)*, May 2017, pp. 1037–1040. doi: 10.1109/RADAR.2017.7944357.
- [5] M. Krátký and L. Fuxa, 'Mini UAVs detection by radar', in *International Conference on Military Technologies (ICMT) 2015*, May 2015, pp. 1–5. doi: 10.1109/MILTECHS.2015.7153647.
- [6] A. Moses, M. J. Rutherford, and K. P. Valavanis, 'Radar-based detection and identification for miniature air vehicles', in *2011 IEEE International Conference on Control Applications (CCA)*, Sep. 2011, pp. 933–940. doi: 10.1109/CCA.2011.6044363.
- [7] F. Christnacher *et al.*, 'Optical and acoustical UAV detection', in *Electro-Optical Remote Sensing X*, Oct. 2016, vol. 9988, p. 99880B. doi: 10.1117/12.2240752.
- [8] T. Zsedrovits, A. Zarandy, B. Vanek, T. Peni, J. Bokor, and T. Roska, 'Visual Detection and Implementation Aspects of a UAV See and Avoid System', in *2011 20th European Conference on Circuit Theory and Design (ECCTD)*, Aug. 2011, pp. 472–475. doi: 10.1109/ECCTD.2011.6043389.
- [9] D. Bratanov, L. Mejias, and J. J. Ford, 'A vision-based sense-and-avoid system tested on a ScanEagle UAV', in *2017 International Conference on Unmanned Aircraft Systems (ICUAS)*, Jun. 2017, pp. 1134–1142. doi: 10.1109/ICUAS.2017.7991302.
- [10] E. E. Case, A. M. Zelnio, and B. D. Rigling, 'Low-Cost Acoustic Array for Small UAV Detection and Tracking', in *2008 IEEE National Aerospace and Electronics Conference*, Jul. 2008, pp. 110–113. doi: 10.1109/NAECON.2008.4806528.
- [11] A. Finn and S. Franklin, 'Acoustic sense avoid for UAV's', in *2011 Seventh International Conference on Intelligent Sensors, Sensor Networks and Information Processing*, Dec. 2011, pp. 586–589. doi: 10.1109/ISSNIP.2011.6146555.
- [12] B. Harvey and S. O'Young, 'Acoustic Detection of a Fixed-Wing UAV', *Drones*, vol. 2, no. 1, Art. no. 1, Mar. 2018, doi: 10.3390/drones2010004.
- [13] M. Hammer, M. Hebel, M. Laurenzis, and M. Arens, 'Lidar-based detection and tracking of small UAVs', in *Emerging Imaging and Sensing Technologies for Security and Defence III; and Unmanned Sensors, Systems, and Countermeasures*, Oct. 2018, vol. 10799, p. 107990S. doi: 10.1117/12.2325702.
- [14] D. Klarer, A. Domann, M. Zekel, T. Schuster, H. Mayer, and J. Hennig, 'Sense and Avoid Radar Flight Tests', in *2020 21st International Radar Symposium (IRS)*, Oct. 2020, pp. 19–23. doi: 10.23919/IRS48640.2020.9253744.
- [15] D. Klarer, S. Beer, and P. Feil, 'Radar demonstrator for airborne Sense Avoid', in *2017 18th International Radar Symposium (IRS)*, Jun. 2017, pp. 1–7. doi: 10.23919/IRS.2017.8008091.
- [16] M. P. Owen, S. M. Duffy, and M. W. M. Edwards, 'Unmanned aircraft sense and avoid radar: Surrogate flight testing performance evaluation', in *2014 IEEE Radar Conference*, May 2014, pp. 0548–0551. doi: 10.1109/RADAR.2014.6875652.
- [17] G. Roos, 'Infineon simplifies 24-GHz radar sensing with three demo kits', *Electronic Products*, Jul. 01, 2019. <http://www.electronicproducts.com/infineon-simplifies-24-ghz-radar-sensing-with-three-demo-kits/> (accessed Jan. 21, 2021).
- [18] 'Impulse Technologies Releases Anteral's 24 GHz uRAD Radar | 2020-12-30 | Microwave Journal'. <https://www.microwavejournal.com/articles/35209-impulse-technologies-releases-anterals-24-ghz-urad-radar> (accessed Jan. 22, 2021).
- [19] 'Multi-Channel Radar Modules for 24 GHz ISM Band | 2018-02-15 | Microwave Journal'. <https://www.microwavejournal.com/articles/29713-multi-channel-radar-modules-for-24-ghz-ism-band> (accessed Jan. 22, 2021).
- [20] B. Mencia-Oliva, J. Grajal, and O. A. Yeste-Ojeda, 'COTS technologies for radar sensors at millimeter-wave bands', in *2011 IEEE MTT-S International Microwave Workshop Series on Millimeter Wave Integration Technologies*, Sep. 2011, pp. 105–108. doi: 10.1109/IMWS3.2011.6061849.
- [21] Infineon, 'BGT24MTR11 datasheet, Rev. 3.1',.
- [22] M. Skolnik I., 'Introduction to Radar Systems', *Sens. Rev.*, vol. Vol. 19 No, no. radar, pp. 1–539, 1999, doi: <https://doi.org/10.1108/sr.1999.08719bae.001>.
- [23] International Association of Marine Aids to Navigation and Lighthouse Authorities, *Preparation of Operational and Technical Performance Requirements*, 1st ed., no. May. France, 2015.